Developing an universal TFIH Equipment using 3D Eddy Current Field Computation

Dietmar Schulze and Zanming Wang
Technical University of Ilmenau, 98684 Ilmenau, Germany
Bernard Nacke
ABB Industrietechnik AG , 44147 Dortmund, Germany

Abstract—**The application of 3D FEM computation of quasi-static eddy current field and its coupled thermal, force field in developing an universal Transverse Flux Induction Heating (TFIH) equipment used for heating thin slabs in Thin-Slab-Casting-Processes(TSCP) is described in this paper. The A+ϕ formulation with Coulomb Gauge is applied and the continuity condition of the current is verified. The ICCG method is used for solving the algebraic system of equations. Fourier's thermal conduction equation for moving media is computed. The computed results are confirmed by measurement at a TFIH equipment. By the arrangement optimization of the equipment for the required temperature distribution a concise optimal method named Orthogonal Experimental Design is applied.**

I. Technological Problem

The more and more stringent requirements in the designing of the modern induction heating equipment, which must be operated under high power density at minimum cost and optimal efficiency or for a required technical parameter with maximal efficiency during operation, necessitate accurate performance prediction of the process. Induction heating processes for heating plates, strips and thin slabs offer significant technological, economic and ecological advantages as comparing with conventional gas-fired plants. For Thin-Slab-Casting-Processes(TSCP) in modern iron and steel making and metal thermal processing industry, an universal induction heating equipment is needed to heat the workpiece which has different temperature distributions before the processing and different technical heating demands as well as different workpiece dimensions and materials. TFIH [1] has the following advantages over the conventional Axial Flux Induction Heating (AFIH) with lower frequencies, less reactive power and laterally open inductor's design. Another important advantage of the new TFIH method - the adaptability of the heating process along the width of the slab according to the incoming temperature profile - allows a flexible reheating of the thin slab to homogenous temperature distribution and the temperature compensation to underheating of the cold edges of the slab because of thermal radiation and convection. A 3d FEM multi-field simulation under real working conditions must be used for developing such equipment, see Fig. 1. In order to get a required temperature-time profile in the development a practical and efficiently optimal method: Orthogonal Experiment Design [2] is applied, which is particularly beneficial for the optimization of a large, complex processes.

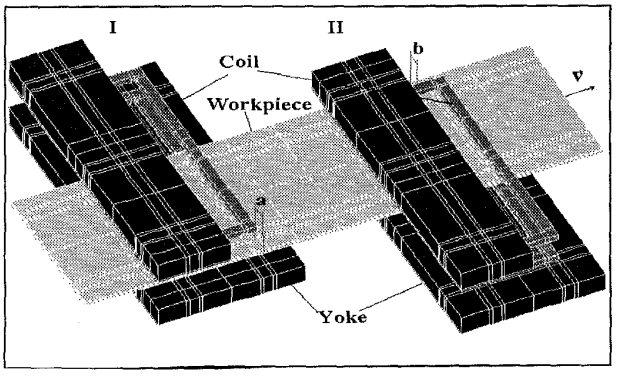

Fig.1 Optimizations model of the TFIH Equipment
(only one half of upper yokes are illustrated)

Manuscript received July 10,1995

II. Mathematical Model

The mathematical model for this sinusoidal quasi-static eddy current problem results from the Maxwell equations and is described by means of the complex magnetic vector potential $\underline{\vec{A}}$ and a complex scalar potential $\underline{\phi}$ [3]. In the middle frequency domain, the effect of the moving of the workpiece with speed <1m/s to electromagnetic field is negligible.

$$\mathrm{rot}\frac{1}{\mu}\mathrm{rot}\,\underline{\vec{A}} - \mathrm{grad}\frac{1}{\mu}\mathrm{div}\,\underline{\vec{A}} + j\,\omega\,\kappa\left(\underline{\vec{A}} - \mathrm{grad}\,\underline{\phi}\right) = \kappa\,\underline{\vec{E}}_s \quad (1)$$

$\vec{E}_s$ is the electric field strength impressed by the power source. Moreover, the requirement of a zero divergence condition of current density must be fulfilled:

$$\mathrm{div}\left(\omega\,\kappa\,\underline{\vec{A}} - \omega\,\kappa\,\mathrm{grad}\,\underline{\phi}\right) = 0 \quad (2)$$

The eddy current density is computed with (3).

$$\underline{\vec{J}} = \mathrm{j}\,\omega\,\kappa\left(\underline{\vec{A}} - \mathrm{grad}\,\underline{\phi}\right) + \kappa\,\underline{\vec{E}}_S \quad (3)$$

The scalar potential $\underline{\phi}$ plays an important role in meeting the needs of the continuity condition of the current at the interfaces.

The current density determines the heat source distribution.

$$p_V = \underline{\vec{J}} \cdot \underline{\vec{J}}^* / \kappa \quad (4)$$

By the numerical investigations it is shown that the introduction of the scalar potential $\underline{\phi}$ is indispensable, if the solution is uniquess and the zero divergence condition of current density must be fulfilled, particularly by the inductor protruding beyond the strip edge.

The temperature field $\vartheta(x, y, z)$ is computed on the basis of the Fourier's thermal conduction equation.

$$\frac{\partial(c\rho\vartheta)}{\partial t} = \operatorname{div}(\lambda \operatorname{grad}\vartheta) + p_V - \vec{v}\operatorname{grad}(c\rho\vartheta) \qquad (5)$$

wherein λ is the thermal conductivity coefficient, c specific heat, ρ mass density and $\vec{v}$ strip velocity respectively, p_V shown in (4), the term $\vec{v}\operatorname{grad}(c\rho\vartheta)$ shows the change of the heat source resulted from the moving of the strip.

Forces which can be calculated using the computed field variables $\vec{A}$ and $\vec{J}$ act through the electromagnetic field on the strip. Only the Lorentz force acts on a non-ferromagnetic workpiece. The force $\vec{F}_V$ related to the unit of volume can be split into a mean value and a portion oscillating at twice the inductor current frequency.

$$\vec{F}_V = \operatorname{Re}\left\{\vec{J}\times(\operatorname{rot}\vec{A})^*\right\} + (\vec{J}\times\operatorname{rot}\vec{A})\cos(2\omega t) \qquad (6)$$

III. Numerical Model

The computation of the electromagnetic field by approximation is performed on the basis of the finite element method. The Galerkin method is applied to (1) and (2), duly considering the boundary and symmetry conditions. The ICCG method is used for solving the global algebraic system of equations. The material characteristic is supposed to be constant by the eddy current computation; Regarding the time consumed by considering the interaction between the electromagnetic and the thermal field the interaction is omitted.

The computation of the temperature field of the moving strip is done on the basis of a particular grid. The heat source distribution, which was calculated with (4) in eddy current computation in the form of node values, is transferred to this grid (which can not be identical with the grid of the electromagnetic computation) by means of the shape functions. Thermal losses by convection and radiation on the strip surface are duly considered. On the side on which the strip enters the solution area, temperatures (e.g. ambient temperature) are given. On the exit side, however $\partial\vartheta/\partial x = 0$ (the x coordinate corresponds to the velocity direction) is indicated. The influence of the velocity destroys the coefficient matrix symmetry of the equation system. A biconjugate gradient procedure or a relaxation procedure was therefore adopted as the solution method. Test computations revealed that a better stability is accomplished by transient computation, therefore the Cranck-Nicolson method was applied.

IV. Simulation

Fig. 2 shows the mesh of the inductor (coil), yoke and strip (airfilled spaces is not shown). 82544 hexahedral elements with 89148 nodes resulted for the 1/2 of the overall computation domain.

The results presented below relate to this specific example which is one of many modifications. In Fig. 3 the calculated eddy current distribution on the strip surface is illustrated. Because the depth of current penetration is much greater than the strip width, a similar eddy current distribution will also occur in the deeper layers.

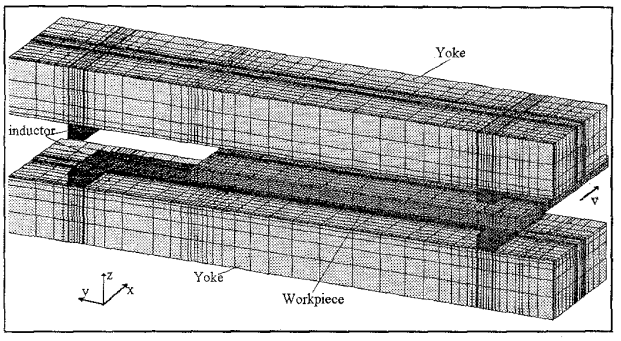

Fig. 2 Finite element mesh of the 1/2 equipment.

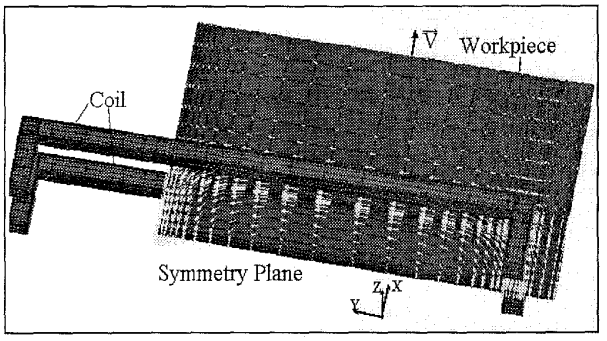

Fig. 3 Eddy current distribution on the strip surface(no yoke)

If the workpiece is wide enough, the eddy current flows normally along and under the inductor in the workpiece. In Fig. 3 one can see that the eddy current is forced to flow only within the workpiece, although the inductor protrudies beyond the workpiece edge. Because at the long inductor side and under it the eddy current density is very high and therefore leads to overheating. The comparison of power density distributions for a long (computation example) and a short inductor shown in Fig. 4 indicates the possible combinations, configurations and geometries by which a desired final temperature distribution can be obtained.

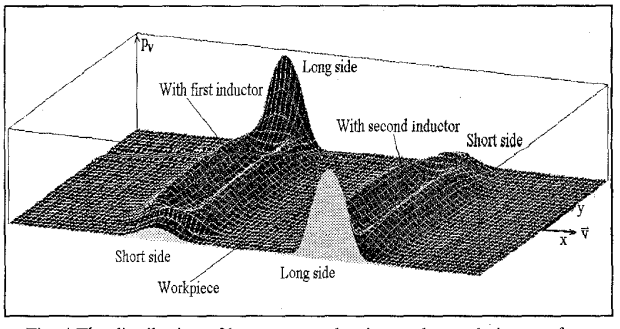

Fig. 4 The distribution of heat sources density on the workpiece surface

Fig. 5 shows the temperature distribution resulting from the reflected heat sources density in Fig. 4, which is calculated with (4).

The computed results are confirmed by temperature measurements performed with an infrared camera. Fig. 6 shows a comparison between them at the outlet side, the close agreement verifies the accuracy of the above models. Fig. 7 shows the force density distribution on planes, yz with x=0 and xy with z=.0025m.

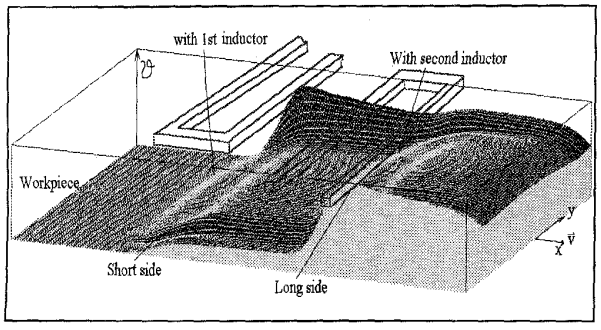

Fig. 5. Steady-state temperature distribution.

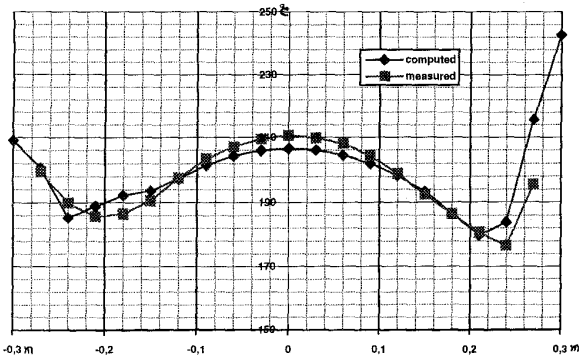

Fig. 6 Temperature distribution across the strip width at the outlet side.

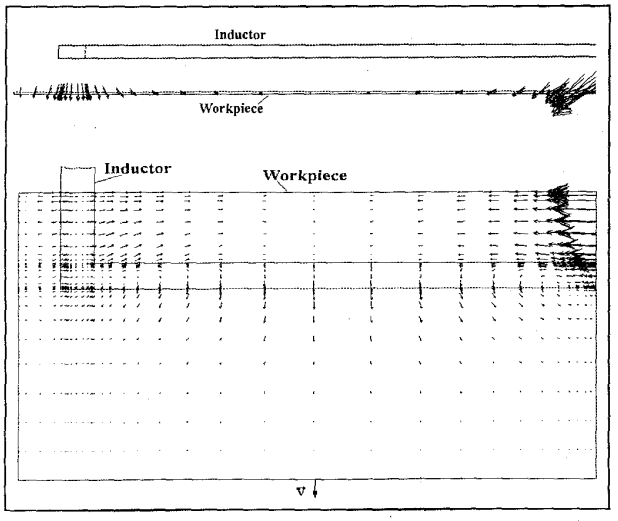

Fig. 7 Force density distribution on planes, yz with x=0 (top) and xy with z=.0025m.

V. Optimization

The primary objective of optimization is to accomplish a definite temperature distribution over the strip cross section downstream of the inductor outlet. The technological problem definition specifies different temperature distributions at the inductor inlet as well as different workpiece dimensions and materials. The objective of optimization can be influenced by the number of poles (inductors), their geometric shape (inductor, yoke), the power source frequency and the different arrangement of the inductors. Because the geometry of the inductor was already determined, here only the optimization of the minimum temperature difference between the given and the calculated temperature for a thin slab of 0.6 m width is carried out.

An exact analysis of the coupled electromagnetic and thermal process needs a 3d FEM eddy current and temperature fields computation. For a whole computation needs normally one day including: meshing for electromagnetic field, the computation of the 3d eddy current field, the conversion of the mesh and the induced heat source for temperature field and the computation of the temperature fields with moving workpiece. So it is hardly possible to optimise the process with classical optimization methods, which needs normally over 100 such FEM computations.

The classical experimental approach, e.g. one-variable-at-a-time method is to study each experimental variable separately, in that there are almost always a large number of variables and each experiment lasts a long time. So it is necessary to reduce the number of trials and time-consumption. Experimental designs can be used to study a great number of factors while keeping total number of trials within reason. It uses statistics as a foundation emphasizes engineering judgement. For each level of any one factor, all levels of the factors occur an equal number of times. This constitutes a balanced experiment and permits the effect of one factor under study to be separable from the effects of other factors. Although balanced, the design of an orthogonal array does not require that all combinations of all factors be tested. Therefore, the experimental matrix can be smaller without losing any vital information. An additional advantage is their cost efficiency. Here the experimental design and computer simulations were combined.

The optimization is carried out with the method named orthogonal experimental method $L_4(2^{**}3)$ [2], it means for 3 variables each with 2 levels only 4 computations need to be done instead of 8. The variables a and b shown in Fig. 1. Level 1 and level 2 of the variable a and b are 0.048m and 0.064m respectively.

The objective function is

$$\min.\ f_q = \sum_i \left(\frac{\vartheta_i - \vartheta_s}{\vartheta_s}\right)^2 \qquad (7)$$

where i the number of the point with calculated temperature at the outlet side, ϑ_i the temperature at the point i, ϑ_S the given temperature with 200 °C.

Fig.8 shows the results: objective function vs variables, the effect of currents and variable b on objective function are more important. By the level 2 of the current and of the variable b, the level 1 of the variable a the objective function gives the best result. The found optimal result is the combination of the levels a1, b2, c2. Fig. 9

shows the best results of this experiment from the initial step. Fig 10 gives a comparison between the temperature gives a comparison

TABLE I ORTHOGONAL EXPERIMENTAL DESIGN L4(2^3)

No. of the Experiments	Variable a-1st inductor (m)	Variable b- 2th inductor (m)	Currents Arrangement I1(A)/I2(A)
1.	0.048	0.048	2800/3380
2.	0.048	0.064	3380/2800
3.	0.064	0.048	3380/2800
4.	0.064	0.064	2800/3380

TABLE II OBJECTIVE FUNCTION

objective function f_q	level 1	level 2	better level
Variable a	0.1627	0.1998	level 1
Variable b	0.2505	0.1538	level 2
Currents	0.2470	0.1154	level 2

between the temperature profiles before and after the optimization at the outlet side. The optimal result shows much better than the original one according to the objective function, because the temperature distribution is more homogenous and the temperature difference between the maximum and the minimum temperature is smaller than the original one.

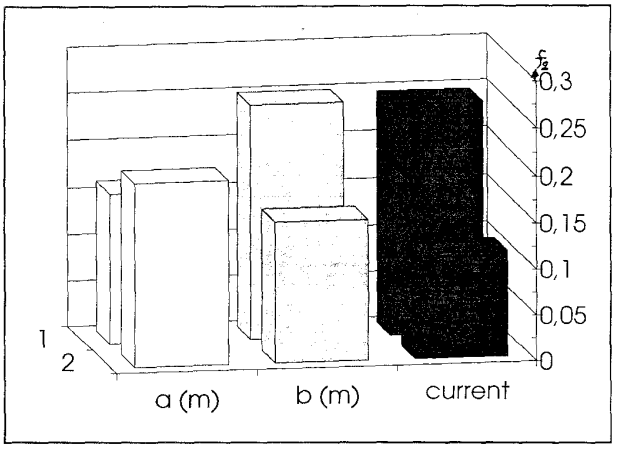

Fig.8 Objective function f_q vs variables

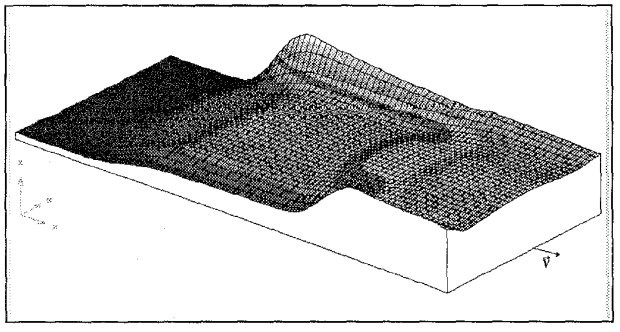

Fig.9 Temperature field distribution after the optimization

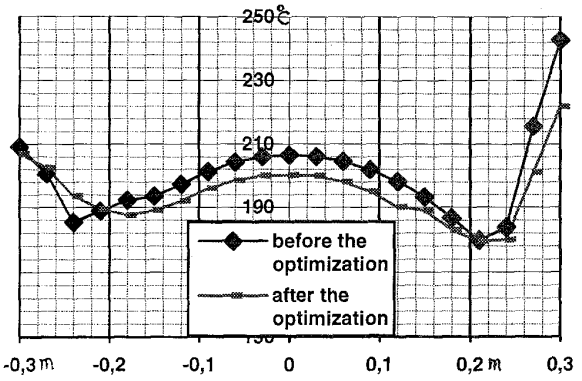

Fig.10 Temperature distribution on outlet side after the optimization

Conclusions

The simulation and the optimization for the Transverse Flux Induction Heating with 3d FEM eddy current field computation based on A+ϕ formulation with Coulomb Gauge and temperature field computation based on Fourier's thermal conduction equation for moving media are successfully carried out and the continuity condition of the current in the computation is guaranteed. The application of ICCG method reduces the time-consuming for solving the algebraic system of equations. The computed results are confirmed by measurement at a TFIH equipment. The orthogonal experimental design method is very useful and effective for such complicated optimization problems. The optimization for minimising the temperature difference at the outlet side gives a good result for the problem.

References

[1] R.M. Baker: AIEE Trans., 69(1950), 711-719

[2] Ch. Maduo, Ch. Kuei, Experimental Statistical Designs and Analysis in Simulation Modelling, Quorum Books. London , 1993

[3] O. Biro, K. Preis, "On the use of the magnetic vector potential in the finite element analysis of three-dimensional eddy currents, " *IEEE Transaction on Magnetic*, vol. 25, No. 4, pp. 3145-59, July 1989.

[4] D. Schulze, Z. Wang and B. Nacke, "Computer simulation of transverse flux induction heating(TFIH) for continuous-thin-slab-casting", Inter. Symp. on EPM, pp. 523-28 , Oct. 1994, Nagoya, Japan.

[5] D. Schulze, Z. Wang and W. Andree, "3d eddy current computation in the transverse flux induction heating equipment", *IEEE Transaction on Magnetic*, vol. 30, pp.3072-75 No. 5, Sept. 1994